



Study of laser texturing assisted abrasive flow finishing for enhancing surface quality and microgeometry of spur gears

Anand C. Petare¹ · Ankit Mishra¹ · I. A. Palani¹ · N. K. Jain¹

Received: 16 July 2018 / Accepted: 26 October 2018 / Published online: 8 November 2018
© Springer-Verlag London Ltd., part of Springer Nature 2018

Abstract

This paper reports on study of laser texturing assisted abrasive flow finishing (LT-AFF) process of the hobbled spur gear (HSG) to further improve their microgeometry, surface finish, microhardness, microstructure, wear resistance, and material removal rate (MRR) as compared to AFF process. Preliminary experiments were conducted to identify optimum values of power and focal length of the continuous fiber laser of 1064-nm wavelength, and number of passes for laser texturing of the HSG made of 20MnCr5 alloy steel. Identified optimum values were used to produce homothetic texture on flank surfaces of HSG in a direction perpendicular to the lay profile generated by hobbing. Influence of laser texturing was studied by comparing deviations in microgeometry, average and maximum surface roughness values, microhardness, wear resistance, and MRR of HSG directly finished by AFF and laser-textured hobbled spur gears (LTHSG) finished by AFF. Previously optimized value of viscosity of AFF medium was used during finishing of HSG and LTHSG. Deviations in total profile, total lead and total pitch, and radial runout were used to indicate deviation in microgeometry of the spur gears. Results reveal that AFF of LTHSG reduced surface roughness and errors in microgeometry and improved microhardness, microstructure, wear resistance, and MRR than direct of AFF of HSG. Improved microgeometry and surface quality of spur gears will lead to their increased operating performance and service life thus reducing their running noise and vibrations and preventing their premature and failures. This research proves that productivity of AFF process can be improved significantly by laser texturing for finishing the spur gears.

Keywords Laser texturing · Homothetic texture · AFF · Hobbing · Spur gears · Microgeometry · Surface roughness · Wear resistance

1 Introduction

Gears constitute positive drives that are used to transmit power and/or motion with or without change in the direction of transmission. Gears which are mounted on the parallel shafts are called cylindrical gears. Spur, single helical, double helical, and herringbone gears belong to this category. Spur gears have simpler design, easy to manufacture, do not have axial thrust, more efficient and precise, and less costly. They are used in high speed and high load application in all types of gear trains for wide range of velocity ratios. Their typical applications include gearbox of automobiles, railways, aircraft, marine engine, rolling mills, cement mills, conveyor and material

handling equipment, agriculture and farm machinery, elevator and lifts, robots, packaging and food processing, printers, toys, clocks and watches, household gadgets, etc. The mechanical efficiency (i.e., ratio of output power to input power) of unfinished spur gears ranges from 92 to 94%, and it increases up to 99% with high quality of surface finish and very good lubrication [1]. Quality of a gear is assessed in terms of deviations in its microgeometry and is expressed in various international standards such as Deutsches Institut für Normung (DIN), International Organization for Standardization (ISO), American Gear Manufacturers Association (AGMA), British Standards Institute (BSI), and Japanese Industrial Standard (JIS). DIN and AGMA are the most frequently used standard for gear quality. In DIN-3961-1 gear quality categorized into 12 groups, DIN 1 is for best quality high accurate gear and DIN 12 poorest quality gear. In ANSI/AGMA 2015-1-A01 gear quality categorized in 10 groups, A2 indicates the best quality high accurate gear and A11 indicating the poorest quality of the gear [2].

✉ N. K. Jain
nkjain@iiti.ac.in

¹ Discipline of Mechanical Engineering, Indian Institute of Technology Indore, Simrol, Indore, MP 453 552, India

Annual consumption of gears is more than two billion for various applications. Therefore, careful design and manufacturing of gears to achieve their highest possible quality at minimum possible cost are very essential. This has motivated researchers to continuously improve manufacturing and finishing processes of different types of gears. Typical manufacturing of gear involves preparation of gear blank, teeth generation, finishing, heat treatment, post-heat treatment finishing, coating, inspection of gear quality, and packaging [3]. Traditional finishing processes for cylindrical gears are shaving, burnishing, skiving, honing, grinding, and lapping. Only gear grinding and lapping are used for finishing conical gears. But, these processes have their own inherent limitations as mention in [4]. It reduces their applicability for wide variety of gear finishing requirements. This has forced researchers to develop non-traditional or advanced finishing process for gear which is able to overcome limitations of the traditional processes, easy to operate, productive, cost-effective, and more importantly gives better quality, surface finish, wear resistance, operating performance, and service life of the gears. In this direction, various advanced finishing processes have been developed recently such as (i) electrochemical honing (ECH) by Shaikh et al. [5] and pulsed-ECH (PECH) by Pathak et al. [6] for straight bevel gears made of electrically conducting materials only, (ii) abrasive flow finishing (AFF) for helical gears by Xu et al. [7], for bevel gears by Venkatesh et al. [8], and for spur gears [9] and straight bevel gears [10] by Petare and Jain, and (iii) ultrasonic assisted AFF (US-AFF) by Venkatesh et al. [11].

Past work on gear finishing by AFF reveals that it has capability to finish different types of gears effectively due to back and forth extrusion of a self-deformable abrasive laden viscoelastic finishing medium (known as putty) through the gaps between two consecutive gear teeth. It enables it to remove nicks, burrs, surface peaks, and gear teeth cutter marks, thus imparting fine finishing to gears. It was found to enhance microgeometry, wear resistance, and microhardness of straight bevel gears [10]. Additionally, it can be used for deburring, radiusing, polishing, surface stress relieving, geometry optimization, and to remove EDM recast layer of components in a wide range of applications. Though AFF offers many advantages for gear finishing, but it suffers from many limitations also. Its worth-mentioning limitations are (i) mixing of the removed material to the finishing medium and subsequent changes in the composition of the medium, (ii) difficulty in predicting increase in temperature during finishing, (iii) prediction and online control of rheological properties of the finishing medium, (iv) unpredictability of movement and distribution of the abrasive particles during finishing and its control, (v) difficulty in determining finishing time of a component and useful life of the AFF medium, and (vi) lower material removal rate (MRR) and consequently longer finishing time. Researchers have developed various

hybrid and derived variants of AFF to overcome some of these limitations to certain extent [12].

Recently, laser texturing has emerged as an effective techno-commercial solution to improve performance of various machining and finishing processes, and to enhance tribological properties and service life of the engineering components. Presence of microtexture improves friction and wear behavior and lubricating properties of critical components which are very important for an engineering component like gear. Due to heat generation in the laser texturing process, melting and ablation of workpiece material are observed. Therefore, subsequent finishing of the workpiece is required to remove the slag and excess molten material so as to achieve the intended surface quality. This finishing can be done using fine abrasive particles in the standard finishing processes. Laser texturing has improved surface properties and reduced coefficient of friction for Ti-6Al-4V alloy, stainless steel, and steel based nitride [13]. Sasi et al. [14] employed laser texturing to high-speed steel (HSS) cutting tool for machining of Al7075-T6 aluminum alloy for aerospace applications and found that it enhanced tribological properties of HSS cutting tool under dry machining condition and reduced the cutting force and thrust force by 9% and 19%, respectively. Kang et al. [15] laser-textured injection cam was made of AISI 1045 steel to improve its anti-wear characteristics for use in internal combustion engines. They reported 30% improvement in anti-wear characteristics of the laser-textured injection cam than the non-textured injection cam. Ye et al. [16] created micro-grooved texture on rack face of cemented carbide tool for turning of C45 steel and reported significant reduction in cutting forces and coefficient of friction as compared to the non-textured tool. Hao et al. [17] generated homothetic and hybrid textures by laser on carbide tool for machining of Ti-6Al-4V titanium alloy and reported 9.3% reduction in coefficient of friction for hybrid texture and 5.8% by homothetic texture as compared to the non-textured tool. Singh et al. [18] used laser for creating micro-patterns and micro-dimples on cellulose acetate film, polyethylene terephthalate, Ti-6Al-4V alloy, and stainless steel (SS 304) to investigate their tribological behavior and contact angle. They found that laser texturing increased the surface roughness which increased contact angle in both metal and polymers and that coefficient of friction reduced from 0.66 to 0.45, 0.18, and 0.17, respectively for low, medium, and high-density area of texture. Niketh and Samuel [19] created micro-texture and micro-dimples by laser on 8-mm diameter carbide drill to make holes in Ti-6Al-4V and reported 12.3% reduction in torque, 10.6% reduction in the thrust force, and formation of less built-up edge (BUE) than that with the non-textured drill tool. Xing et al. [20] created laser texture on Si_3N_4 and TiC ceramics and investigated their anti-wear performance using ball-on-disk tribo-test and used finite element analysis for stress distribution. They concluded that (i) tribological performance is influenced by

size and density of the grooves created by laser, (ii) wavy grooves with large density result in lower coefficient of friction, and (iii) texturing improves stress distribution pattern at the contact edges and reduces concentration of the stress.

It can be concluded from the aforementioned review of the past work that (i) among different types of gears, spur gears are most widely used in different machines, equipment, and applications. But, being their teeth parallel to axes of their mounting shafts leads to sudden engagement and disengagement between their teeth which creating more vibrations and noise particularly for higher speed and higher loads applications, (ii) AFF process has potential to finish different types of gears made of both electrically conducting and non-conducting materials. But, it has certain inherent limitations which restricts its gear finishing performance and productivity, (iii) laser texturing of gears prior to their finishing by AFF has potential to improve finishing performance of AFF process by enabling it to further enhance microgeometry, surface finish, wear resistance, microhardness, and material removal rate of the gears, and (iv) no work has been done on laser texturing assisted AFF (LT-AFF) of spur gears to improve wear resistance, load carrying capacity, operating performance, transmission efficiency, and service life and reduce noise and vibrations. Therefore, present work aims to bridge this gap with the following objectives:

- Using laser texturing to create homothetic texture on flank surfaces of the hobbed spur gears (HSG) in a direction perpendicular to the lay pattern generated by hobbing
- Comparison of finishing performance of AFF on HSG and laser-textured hobbed spur gears (LTHSG) in terms of microgeometry deviations, surface roughness, wear resistance, microhardness, and MRR
- To establish laser texturing as an effective tool for improvement of performance of productivity of AFF to finish gears of higher quality and better surface finish

2 Materials and methods

2.1 Specifications and material of spur gears

The spur gears used in the present study have the following specifications: 3 mm module, 16 teeth, 48 mm pitch circle diameter, 20° pressure angle, 10 mm face width, and 54 mm outside diameter. Alloy steel 20MnCr5 was used as the gear material due to its use in commercial production of spur gears. It has 55 Rockwell hardness value on C-scale (HRC) and chemical composition (by wt%) as 0.8–1.1% Cr, 1–1.3% Mn, 0.14–0.19% C, max. 0.035% P and S, 0.15–0.40% Si and balance Fe.

2.2 Laser texturing

Computer-controlled machine ProMark (from Scantech Laser Pvt. Ltd., Pune, India) having maximum power capacity of 50 W was used to generate 1064-nm wavelength fiber laser. This machine has provision to vary focal length, laser power, and number of passes. Past works [14–20] reveal that most frequently used patterns for laser texturing are homothetic (parallel line), wavy (curved), spot, micro-dimples, micro-pillars of the square, and triangular cross section. Homothetic texture has shown to reduce coefficient of friction by more amount than the other patterns [17]; therefore, it was selected for generation on flank surfaces of all teeth of HSG in a direction perpendicular to the lay pattern generated by hobbing as depicted in Fig. 1a. This resulted in formation of mesh-like structure between homothetic laser textures and lay pattern of hobbing on the flank surfaces of HSG as shown in Fig. 1b, d. This will deflect flow of the abrasives during AFF process providing them random motion, as shown in Fig. 2b, thus enabling them to cover more flow path over the flank surfaces of LTHSG than that on HSG (as shown in Fig.

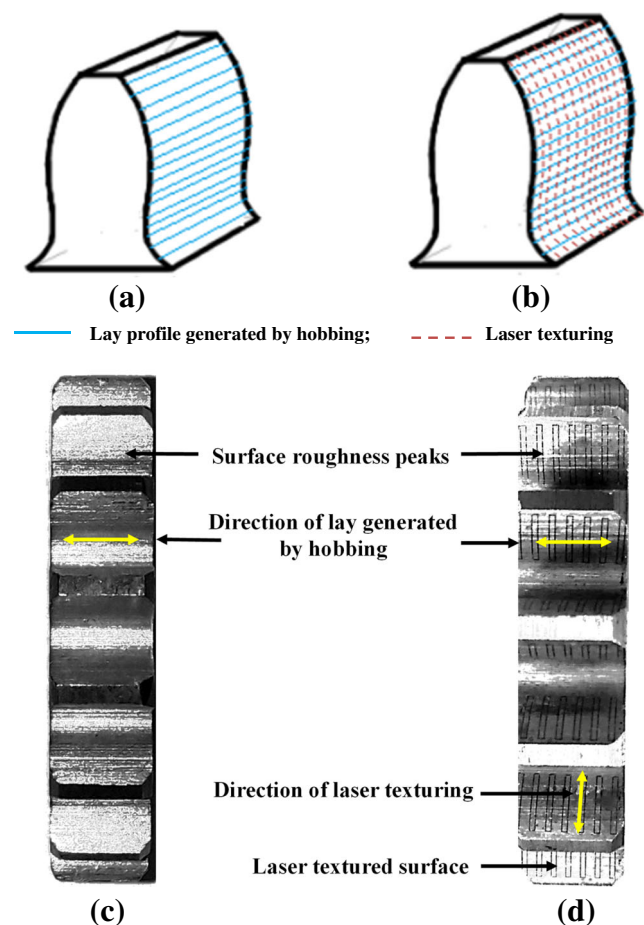


Fig. 1 Schematic of lay profile of a (a) hobbed spur gear (HSG), (b) laser-textured hobbed spur gear (LTHSG), (c) photograph of HSG, and (d) photo of LTHSG obtained using 20-W fiber laser and 5 numbers of passes

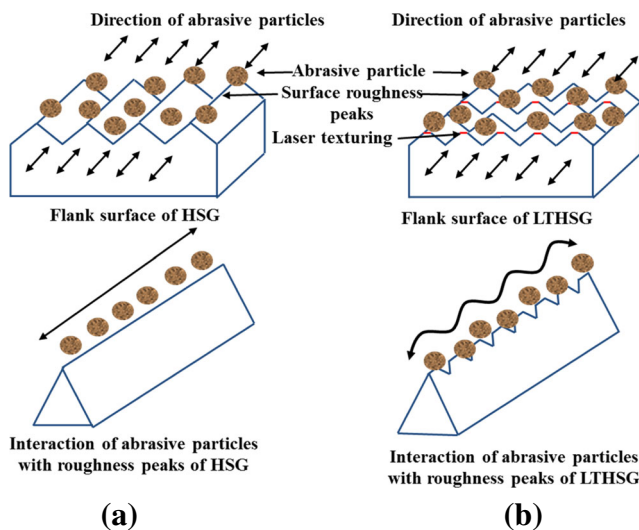


Fig. 2 Schematic of finishing mechanism by AFF process for (a) HSG and (b) LTHSG

2a). This will result in more uniform abrasion and more MRR and consequently less finishing time.

Preliminary experiments were performed to identify optimum values of laser power, focal length, and number of laser passes for generating homothetic laser texture on HSG by varying laser power varied at four levels (i.e., 10, 15, 20, and 25 W), focal length at three levels (i.e., 280 mm, 285 mm, and 290 mm), and numbers of passes at six levels (i.e., 1, 2, 3, 4, 5, and 6). The details of variable and fixed parameters were taken for finding optimum value of laser power and number of passes shown in Table 1.

Optimum value of the focal length was identified according to sharpness of the boundaries and corners of the marking area (product of marking height and length and also known as gain) which is determined according to the size of flank surface of the gear tooth. In the present work, marking height as 2.2 mm and length as 4.4 mm were selected. Figure 3 depicts concept of marking area for focal length value of 280 mm

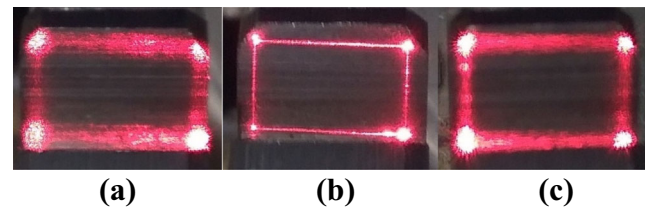


Fig. 3 Concept of boundaries of the marking area on the flank surface of spur gear for laser texturing at different values of focal length: (a) 280 mm, (b) 285 mm, and (c) 290 mm

(Fig. 3a), 285 mm (Fig. 3b), and 290 mm (Fig. 3c) by laser pointer. It is evident that 285 mm focal length yielded very sharp boundaries and corners of the marking area. Therefore, it was identified as optimum value of the focal length. Formation of the laser texture on the flank surfaces of the HSG was checked using the magnifying glass having $\times 10$ magnification. It was observed that no laser texture was formed for laser power < 20 W and number of passes < 5 . Fine laser textures were obtained for the combination of 20-W laser power and 5 number of passes, whereas use of 25-W laser power resulted in burn marks on the flank surfaces of HSG and increased density of texture. Therefore, 20 W as laser power and 5 number of passes were identified as their optimum values for laser texturing of the hobbed spur gears.

2.3 Apparatus and fixture for finishing of spur gear by AFF process

An experimental apparatus as shown in Fig. 4 was used to finish HSG by two-way AFF process. It consists of a hydraulic power pack unit which drives pistons of two vertically positioned hydraulic cylinders which are in turn connected to AFF medium-containing cylinders vertically placed opposite to each other. The gear to be finished (i.e., workpiece gear) is mounted in a specially designed fixture placed between the medium containing cylinders. Finishing cycle in AFF process consists of forward and backward strokes. At the start the forward stroke, the bottom-located medium containing cylinder is filled with a viscoelastic self-deformable AFF medium which is extruded through the flow passages provided between the workpiece and the fixture. During the backward stroke, the top-located medium-containing cylinder extrudes back the AFF medium through the same flow passages. This process continues either for predefined number of finishing cycles or finishing time or surface roughness value. Finishing results of AFF process are highly influenced by design of the fixture because it not only support and holds the workpiece gear but also provides necessary restriction and passages for movement of the viscoelastic AFF medium. A special fixture was designed and developed to finish the spur gears by AFF process (Fig. 5). It consists of two metalon (which is a type of thermoplastic type polymer and also known as cast nylon) disc having circumferential holes drilled by 5-mm diameter drill selected according to

Table 1 Details of the parameters used to identify optimum parameters for laser texturing of the hobbed spur gears

Fixed parameters		
Name	Values used in experiments	
Laser wavelength (nm)	1064	
Gain [marking height (mm) \times length (mm)]	1.9 [2.2 \times 4.1]	
Variable parameters		
Name	Values used in experiments	Identified optimum value
Focal length (mm)	280, 285, 290	285
Laser power (watts)	10, 15, 20, 25	20
Number of laser passes	1, 2, 3, 4, 5, 6	5

Fig. 4 Photograph of the experimental apparatus used for finishing hobbed spur gears by AFF process developed by Petare and Jain [9]

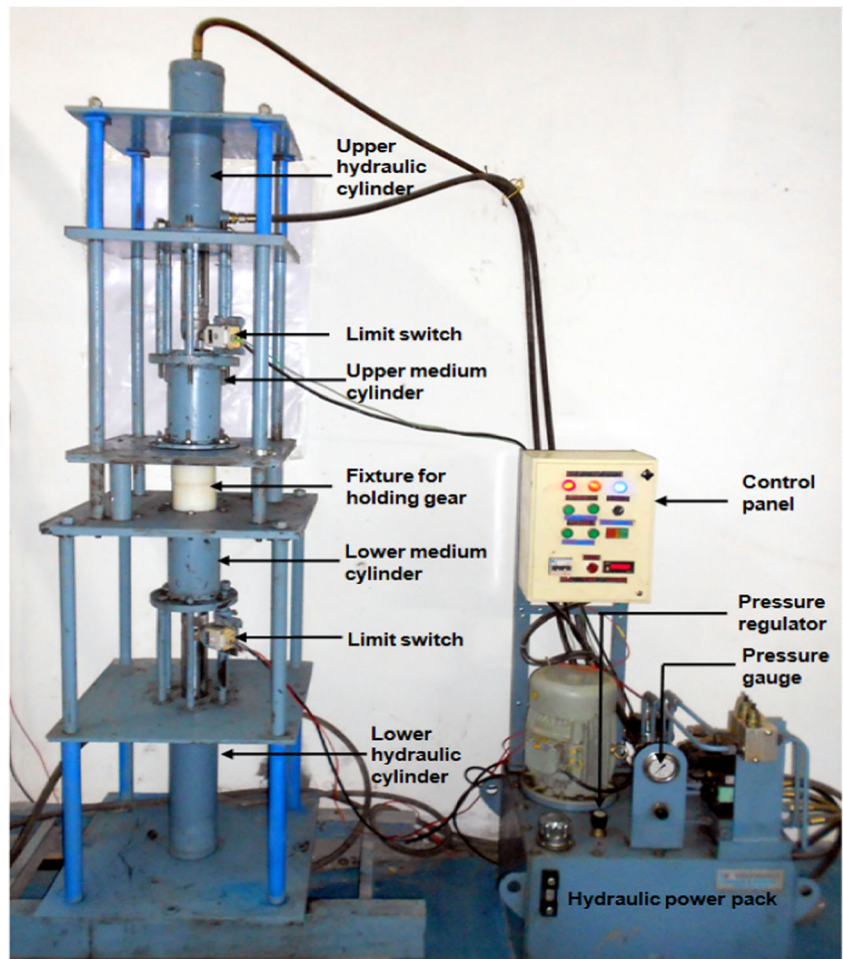
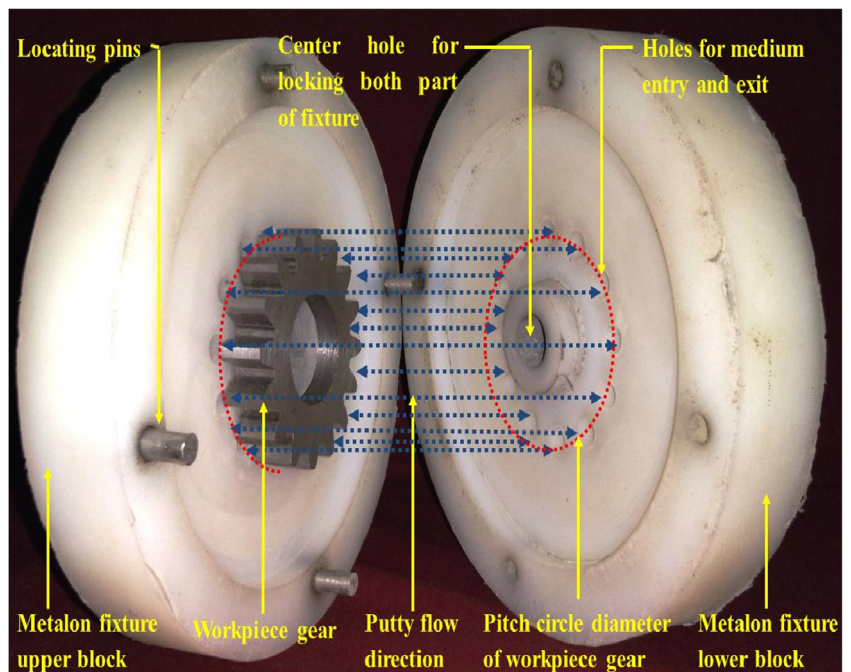


Fig. 5 Photograph of the fixture designed to finish the spur gear by AFF [9]



pitch circle diameter of the gear. A hub is provided in the center of the fixture to hold spur gear firmly and to avoid its rotation when high extrusion pressure is applied during AFF process [9]. The AFF medium passes through these circumferential holes over the flank surfaces during forward and backward strokes of finishing cycles. It causes shearing off the surface roughness peaks along the axial direction (or along the face width) of the gear imparting it fine finish.

3 Details of experimentation

3.1 Process parameters and responses

Viscosity of AFF medium, finishing time, extrusion pressure, type, size and concentration of the abrasive particles, geometry, hardness and chemical composition of the gear material, fixture, and clamping method are significant parameters of AFF process which affects the surface quality and deviations in microgeometry of the AFF finished spur gears. Viscosity of AFF medium η and finishing time t have been considered as the two most important AFF process parameters in achieving the identified objectives of the present work [9, 10].

Gear microgeometry is associated with deviations in form and location of gear teeth. Form deviations are associated with profile and helix, whereas location deviations are associated with pitch and runout. Total profile deviation (F_a) is the sum of deviation in involute form (i.e., difference between theoretical or nominal and actual involute form) and deviation in involute profile angle (i.e., difference between theoretical and actual values of involute angle). Total helix or lead deviation (F_β) is sum of deviation in lead form (i.e., difference between theoretical lead form and actual lead form) and deviation in lead angle (i.e., difference between theoretical helix angle and actual helix angle). Total or cumulative pitch deviation (F_p), also known as *total index deviation*, is the difference between summation of the theoretical values of pitches and summation of the actual values of the pitches over all the teeth of a gear. Radial runout (F_r) is the maximum difference between the actual radial location of all teeth with respect to theoretical radial location of all teeth. Total profile deviation, total helix or lead deviation, total pitch deviation, and radial runout have been used to evaluate deviations in microgeometry of spur gears. Average and maximum surface roughness values have been used to indicate surface finish of spur gears.

3.2 Procedure of experimentation

Total six spur gears were manufactured by hobbing process. Three gears were directly finished by AFF process for finishing duration of 15, 20, and 25 min. Whereas three spur gears were laser-textured (i.e., LTHSG) using the identified optimum parameter of fiber laser and then finished by AFF process for the same finishing duration. AFF medium is a mixture of abrasive particles, viscoelastic putty, and blending oil. Silicon carbide was selected as the abrasive to finish spur gear made of 20MnCr5 alloy steel having 55 HRC. Molding clay (referred as *silly putty*) was selected as putty material due to its good ability to hold the AFF medium together, low cost, and easy availability. Silicon oil was used as blending oil because it helps in easier control over viscosity of the AFF medium. The AFF medium was prepared by mixing the abrasive particles with the putty and blending oil. Viscosity of the prepared AFF medium was measured by rheometer (MCR-301 from AntonPaar, Germany). Previously optimized value 135 kPa/s (corresponding to 10% silicon oil) was used as viscosity of the AFF medium which had 30% volumetric concentration of 100 mesh size SiC abrasives and remaining volume as *silly putty* in 1156 cm³ volume of medium-containing cylinder [9]. Extrusion pressure of 5 MPa was used to extrude the AFF medium back and forth for the selected finishing duration. Surface roughness profile, microhardness, microstructure, and wear characteristics of those HSG and LTHSG were studied which have shown maximum improvement in the considered parameters of microgeometry deviation and surface roughness.

3.3 Measurement of microgeometry deviations

Microgeometry parameters were measured on the computer numerically controlled (CNC) gear metrology machine (SmartGear 500 from *Wenzel GearTec*, Germany) using 3-mm diameter probe. Measurements were taken on left hand (LH) and right hand (RH) flanks of four randomly chosen teeth (of all 16 teeth) of the selected spur gear before and after its finishing by AFF process, and their arithmetic mean was used to compute average percentage improvement in total profile deviation and total lead deviation (average percentage improvement in total pitch deviation) using Eq. 1. Values of runout before and after finishing by AFF were used to calculate percentage improvement in the radial runout PIF_r ,

$Avg.PIF_a$ (or $Avg.PIF_\beta$ or $Avg.PIF_p$)

$$= \frac{Avg.F_a \text{ (or } F_\beta \text{ or } F_p) \text{ before AFF} - Avg.F_a \text{ (or } F_\beta \text{ or } F_p) \text{ after AFF}}{Avg.F_a \text{ (or } F_\beta \text{ or } F_p) \text{ before AFF}} 100(\%) \quad (1)$$

3.4 Measurement of surface roughness

Average and maximum surface roughness values of HSG before and after finishing by AFF were measured on LD-130 (MarSurf from *Mahr Metrology*, Germany) using tracing probe of 10- μm tip diameter and using 2 mm as evaluation length, 0.8 mm as cut-off length, and Gaussian

filter to distinguish between roughness and waviness. Measurements were taken at left and right flank surfaces of randomly chosen tooth of a spur gear, and arithmetic mean of the measured values was used in computing percentage improvement in average and maximum surface roughness, i.e., PIR_a and PIR_{max} using the following equation:

$$\text{Avg. } PIR_a (\text{or Avg. } PIR_{max}) = \frac{\text{Avg. } R_a (\text{or } R_{max}) \text{ before AFF} - \text{Avg. } R_a (\text{or } R_{max}) \text{ after AFF}}{\text{Avg. } R_a (\text{or } R_{max}) \text{ before AFF}} 100(\%) \quad (2)$$

3.5 Assessment of wear resistance

Reciprocating wear tests were performed on the randomly selected one tooth of the (i) HSG before finishing, (ii) best finished HSG by AFF, and (iii) best finished LTHSG by AFF using fretting tribometer CM-9104 (from Ducom, India). The specimens were prepared by cold mounting the selected gear tooth for fixing it in the vice of the tribometer. Facing was done on bottom surface of the cold mount to keep top surface of the gear tooth perfectly parallel to surface of the 5-mm diameter stainless steel ball used in the wear test. Load of 50 N, frequency of 20 Hz, and sliding distance of 5 mm were used as per ASTM G133–05 [21]. Schematic of the fretting wear test performed on the flank surface of LTHSG tooth is shown in Fig. 6. Specific wear rate was calculated using the following relation given by Archard's [22].

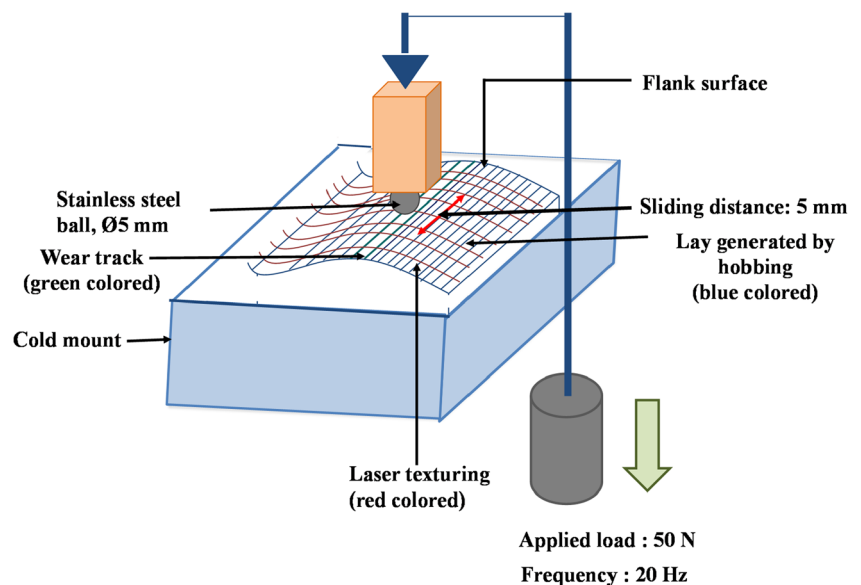
$$k = \frac{V}{Fs} \quad (\text{mm}^3/\text{Nm}) \quad (3)$$

where k is the specific wear rate (mm^3/Nm), V is the wear volume (mm^3), F is the applied load (N), and s is the total sliding distance covered in 20-min duration of the wear test (m). A precision weighing balance having least count 0.001 mg used to calculate mass loss during the wear test from which wear volume was computed.

3.6 Study of microstructure and microhardness

Microstructure and microhardness of the flank surface of randomly selected tooth of (i) HSG before finishing, (ii) best finished HSG by AFF, and (iii) best finished LTHSG by AFF were studied to understand their wear behavior and finishing mechanism. Scanning electron micrographs were taken by field emission SEM Supra 55 (from *Carl-Zeiss NTS GmbH*, Germany). Vicker's microhardness tester VMH-002 (from *Walter UHL*, Germany) was used to determine microhardness value by applying load of 50, 100, and 200 (gm) for a time duration of 15 s as per procedure

Fig. 6 Schematic of fretting wear test performed on the flank surface of LTHSG tooth



prescribed in ASTM E92-82 [23]. Three indentations for each load were taken, and their average value was used for investigation.

3.7 Evaluation of material removal rate

Weight of spur gear before and after finishing by AFF was measured using precision weighing balance DS-152 (*Esaee Teraoka*, Bangalore, India) having least count of 1 mg. Weight measurements were taken three times, and the arithmetic mean of the measured values was used to evaluate *MRR* using following relation

$$MRR = \frac{\text{Avg. value of weight before AFF} - \text{Avg. value of weight after AFF}}{\text{AFF finishing time}} \quad (4)$$

4 Results and discussion

Table 2 presents results of the considered responses for HSG and LTHSG at three values of AFF finishing time. The following observations can be made:

- AFF finished LTHSG yielded higher improvements in parameters of metrology deviations and surface roughness, and *MRR* than AFF finished HSG for three values of AFF finishing time.
- AFF finishing time of 25 min gave maximum values of all the responses for both HSG and LTHSG, i.e., avg. PIF_a as 21.55% and 28.49%; avg. PIF_β as 38.97% and 40.20%; avg. PIF_p as 15.95% and 24.85%; PIF_r as 3.93% and 4.8%; avg. PIR_a as 61.27% and 69.12; avg. PIR_{max} as 48.14% and 68.92%; and *MRR* as 50 and 66 mg/min, respectively. These HSG and LTHSG were considered as the “best finished” for further study of microstructure, microhardness, and wear characteristics.

Figure 7 graphically depicts effect of AFF finishing time on average percentage improvements in total profile deviation PIF_a and total lead deviation PIF_β (Fig. 7a), total pitch deviation PIF_p and percentage improvement in radial runout PIF_r (Fig. 7b), average percentage improvements average and maximum surface roughness PIR_a and PIR_{max} (Fig. 7c), and *MRR* (Fig. 7d) by means of second-order polynomials fitted to the experimental results. The following inferences can be made from these graphs:

- Average PIF_a , avg. PIF_β , avg. PIF_p , PIF_r , avg. PIR_a , avg. PIR_{max} , and *MRR* continuously increases with AFF finishing time and attain their maximum value at 25 min for both HSG and LTHSG, except avg. PIF_p for HSG. This is due to the fact that during early stage of finishing, presence of the highest surface roughness peaks is more on the gear teeth flank surfaces (caused due to hobbing cutter marks, burrs, and nicks) and the abrasive particles try to flatten only these highest surface roughness peaks resulting in lesser amount of contact of abrasives with the surface being finished. This results in less improvement in *MRR*, and the considered parameters of microgeometry deviations and surface roughness. Improvement rate pickup during 20–25 min finishing time because of reducing variation in peak to valley height which results in more abrasives contacting the surface being finished.
- The values of *MRR* and considered parameters of microgeometry deviations and surface roughness for LTHSG are higher than those of HSG at every value of AFF finishing time. This can be explained with the help of mechanism of finishing of HSG and LTHSG by AFF. During finishing of HSG by AFF, the abrasive particles contained in the AFF medium follow straight path along the lay pattern generated by the hobbing process as depicted in Fig. 2a. This reduces length traveled by the abrasive particles causing less number of surface roughness peaks coming in contact with them. It results in lower

Table 2 Values of *MRR*, percentage improvement in microgeometry, and surface roughness parameters of HSG and LTHSG for different values of finishing time

Exp. no.	AFF finishing time <i>t</i> (min)	Gear type	Average percentage improvement in (except in radial runout)						<i>MRR</i> (mg/min)
			Total profile deviation PIF_a	Total lead deviation PIF_β	Total pitch deviation PIF_p	Radial runout PIF_r	Avg. surface roughness PIR_a	Max. surface roughness PIR_{max}	
1	15	HSG	6.89	9.08	2.71	1.24	31.25	26.51	15
		LTHSG	9.34	11.67	6.09	1.94	46.37	36.79	30
2	20	HSG	9.58	20.05	11.26	2.62	46.52	44.06	31
		LTHSG	16.59	27.47	15.64	3.44	51.21	51.23	49
3	25	HSG	21.55	38.97	15.95	3.93	61.27	48.14	50
		LTHSG	28.49	40.20	24.85	4.80	69.12	68.92	66

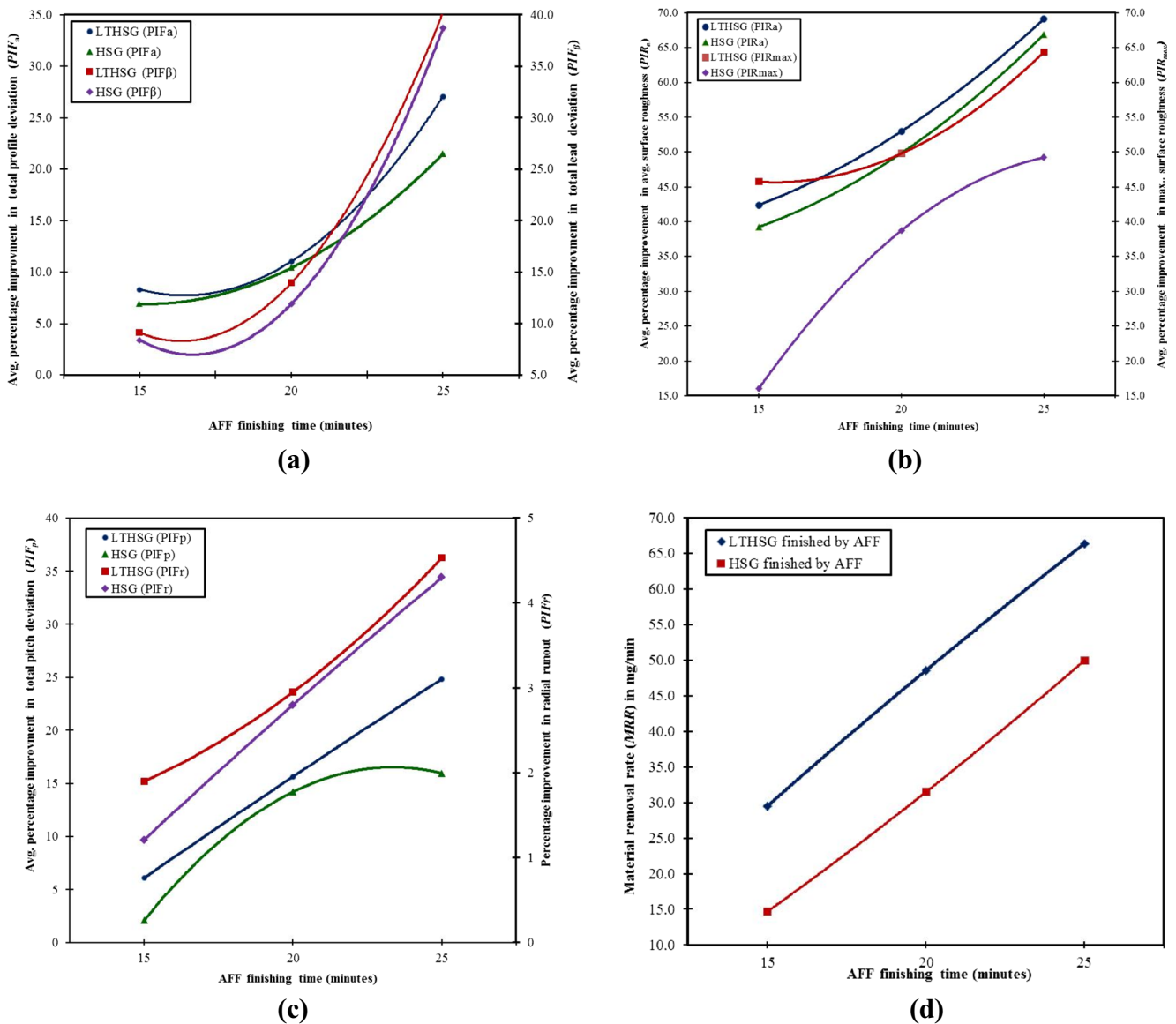


Fig. 7 Variation of percentage improvements in (a) avg. total profile deviation PIF_a and avg. total lead deviation PIF_β , (b) avg. total pitch deviation PIF_γ and radial runout PIF_δ , (c) average surface roughness

PIR_a and maximum surface roughness PIR_{max} , and (d) material removal rate MRR , with AFF finishing time for HSG and LTHSG

improvement in MRR, and parameters of surface roughness and microgeometry deviations. During finishing of LTHSG by AFF, abrasive particles follow curved path with random motion due to the restrictions created by mesh-like pattern generated by superimposing the laser texturing over the hobbing lay pattern as shown in Fig. 2b. This makes travel of abrasive particles nonlinear causing them to travel more distance over the flank surfaces of LTHSG teeth. It results in more number of surface peaks being finished by the abrasive particles which provide uniform abrasion and more improvement in MRR, and parameters of surface roughness and microgeometry deviations.

Table 3 compares four parameters of microgeometry deviation for the best finished HSG and LTHSG before and after their finishing by AFF process. It can be seen from this table that AFF reduced total profile deviation, total lead deviation, and total pitch deviation values of the best finished HSG from 55 to 43.15 μm , 22.45 to 13.7 μm , and 106.55 to 89.55 μm consequently improving its gear quality from DIN 12 to DIN 11, DIN 11 to DIN 10, and DIN 12 to DIN 11, respectively, in these aspects. Radial runout decreased from 171 to 163.7 μm without any change in quality of HSG. For the best finished LTHSG by AFF, total profile deviation, total lead deviation, and total pitch deviation decreased from 55.80 to 39.90 μm , 24.5 to 14.65 μm , and 117.1 to 88.7 μm , thus improving its

Table 3 Comparison of microgeometry parameters of the best finished HSG and LTHSG

Microgeometry parameter (μm)	Best finished HSG		Best finished LTHSG	
	Before AFF (DIN quality)	After AFF (DIN quality)	Before AFF (DIN quality)	After AFF (DIN quality)
Total profile deviation F_a	55 (12)	43.15 (11)	55.80 (12)	39.90 (11)
Total lead deviation F_β	22.45 (11)	13.7 (10)	24.50 (11)	14.65 (10)
Total pitch deviation F_p	106.55 (12)	89.55 (11)	117.1 (12)	88.7 (11)
Radial runout F_r	171 (> 12)	163.7 (> 12)	179 (> 12)	170.4 (> 12)

quality from DIN 12 to DIN 11, DIN 11 to DIN 10, and DIN 12 to DIN 11, respectively, in these aspects. Radial runout reduced from 179 to 170.4 μm without any change in LTHSG.

Figure 8 illustrates surface roughness profile of the HSG before finishing (Fig. 8a), best finished HSG by AFF (Fig. 8b), HSG used for laser texturing (Fig. 8c), and the best finished LTHSG by AFF (Fig. 8d). AFF considerably reduced average and maximum surface roughness values for both HSG (i.e., from 1.83 to 0.71 μm and 12.79 to 6.64 μm , respectively) and LTHSG (i.e., 1.74 to 0.53 μm and 12.94 to 4.02 μm , respectively).

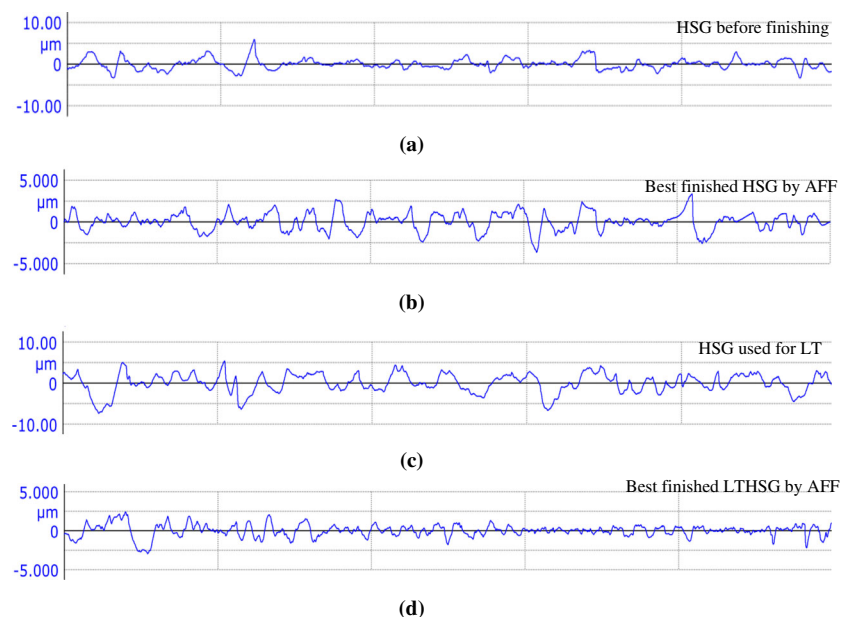
Figure 9 depicts SEM micrographs showing microstructure of flank surfaces of HSG (Fig. 9a), the best finished HSG by AFF (Fig. 9b), and the best finished LTHSG by AFF (Fig. 9c). It can be seen in Fig. 9a that flank surface of HSG has an uneven surface having burrs, pits, hobbing cutter marks, and lay pattern by hobbing. AFF process removes them completely making HSG flank surface very smooth in which some microchips and marks of abrasive flow can be seen (Fig. 9b). The flank surface of best finished LTHSG by AFF is very smooth surface and show marks of only very fine abrasive particles (Fig. 9c).

Presence of marks of abrasive flow and microchips on AFF finished flank surfaces of HSG and LTHSG clearly indicates micro-cutting and micro-plowing mode of material removal followed by the abrading action.

Figure 10 presents results of microhardness test for the HSG, the best finished HSG, and best finished LTHSG by AFF. It can be observed from this figure that the average value of microhardness of the best finished LTHSG by AFF is more than the best finished HSG by AFF which is in turn more than that of HSG before finishing. This can be explained by following phenomena:

- Quenching of laser thermal effect increases microhardness of the laser-textured surface [24].
- Laser induces high-density displacement creating a structure of sub-grain boundary which blocks plastic flow of the material. It also increases microhardness [24].
- High extrusion pressure is used in AFF process to make the finishing medium to flow back and forth over the unfinished surface which removes material through abrasion. Axial and radial forces act on the abrasive particles which increase with the extrusion pressure. Continuous

Fig. 8 Surface roughness profiles of flank surface of (a) HSG before finishing, (b) best finished HSG by AFF process, (c) HSG used for laser texturing, and (d) best finished LTHSG by AFF process



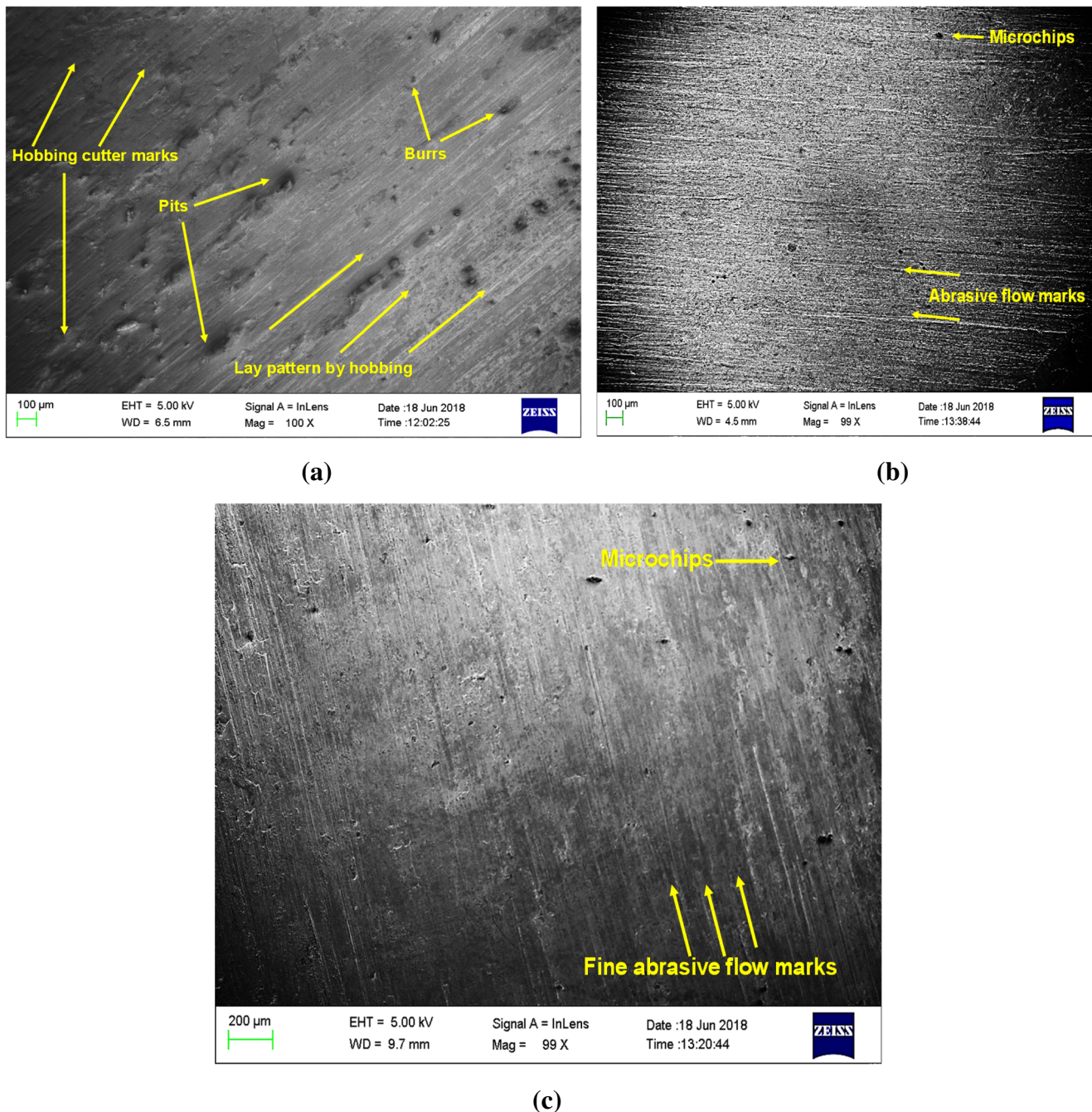


Fig. 9 Microstructure of the flank surface of the (a) HSG, (b) best finished HSG by AFF, and (c) best finished LTHSG by AFF

impact of the abrasive particles results in surface hardening, removal of the fine cracks, burrs, pits, and other surface defects. This increases microhardness of the AFF finished components. It also develops compressive residual stress which improves fatigue strength [25].

All three above-mentioned phenomena are responsible for increasing microhardness of the best finished LTHSG than the best finished HSG and HSG, whereas only last phenomenon is

responsible for increasing microhardness of the best finished HSG than HSG.

Figure 11 shows variation of experimental values of coefficient of friction (Fig. 11a) and friction force (Fig. 11b) with fretting wear time for HSG, the best finished HSG and LTHSG. It is clear from these graphs that (i) coefficient of friction and friction force increases rapidly initially, attains their maximum values, and then stabilizes for HSG and best finished HSG and LTHSG, and (ii) flank surface of HSG shows highest value of coefficient of

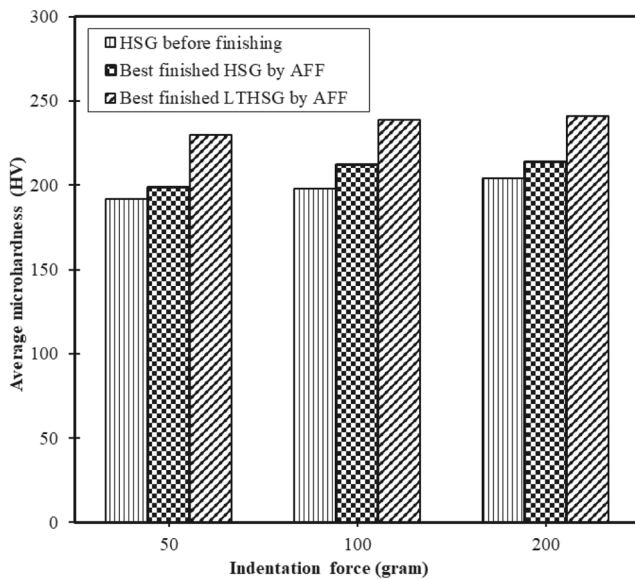


Fig. 10 Comparison of microhardness values for the HSG, the best finished HSG by AFF, and the best finished LTHSG by AFF

friction and friction force among all. Table 4 presents maximum values of coefficient of friction and friction force (obtained from graph of Fig. 11a, b), wear volume obtained from the fretting wear test, and computed values of specific wear rate and wear rate using Eq. 3.

It can be observed from Fig. 11 and Table 4 that (i) maximum values of coefficient of friction and frictional force, wear volume, specific wear rate, and wear rate are significantly decreased after finishing of HSG and LTHSG by AFF, and (ii) reduction in these wear characteristics is more in case of the best finished LTHSG than the best finished HSG. These can be explained by the following:

- HSG before for finishing has large variation in its surface roughness profile as shown in Fig. 8a. This causes less contact area for distribution of the applied force resulting in high coefficient of friction and friction force which result in higher wear rate or lower wear resistance.
- Finishing of HSG and LTHSG by AFF decreases surface roughness, thus smoothing their flank surfaces which increases the contact area for distribution of the applied force. It results in lower coefficient of friction and friction force resulting lower wear volume or more wear resistance.
- The best finished LTHSG has least wear rate and maximum wear resistance because of (i) smoother surface with less variation in roughness profile and (ii) distortion of lattice structure at microscale during laser texturing which forms compressive residual stress [25]. This will result in less heat generation during power transmission, thus reducing operating temperature of the gear drive.

- Very small value of wear volume of the best finished LTHSG than the best finished HSG will enhance its service life and mechanical efficiency [26].

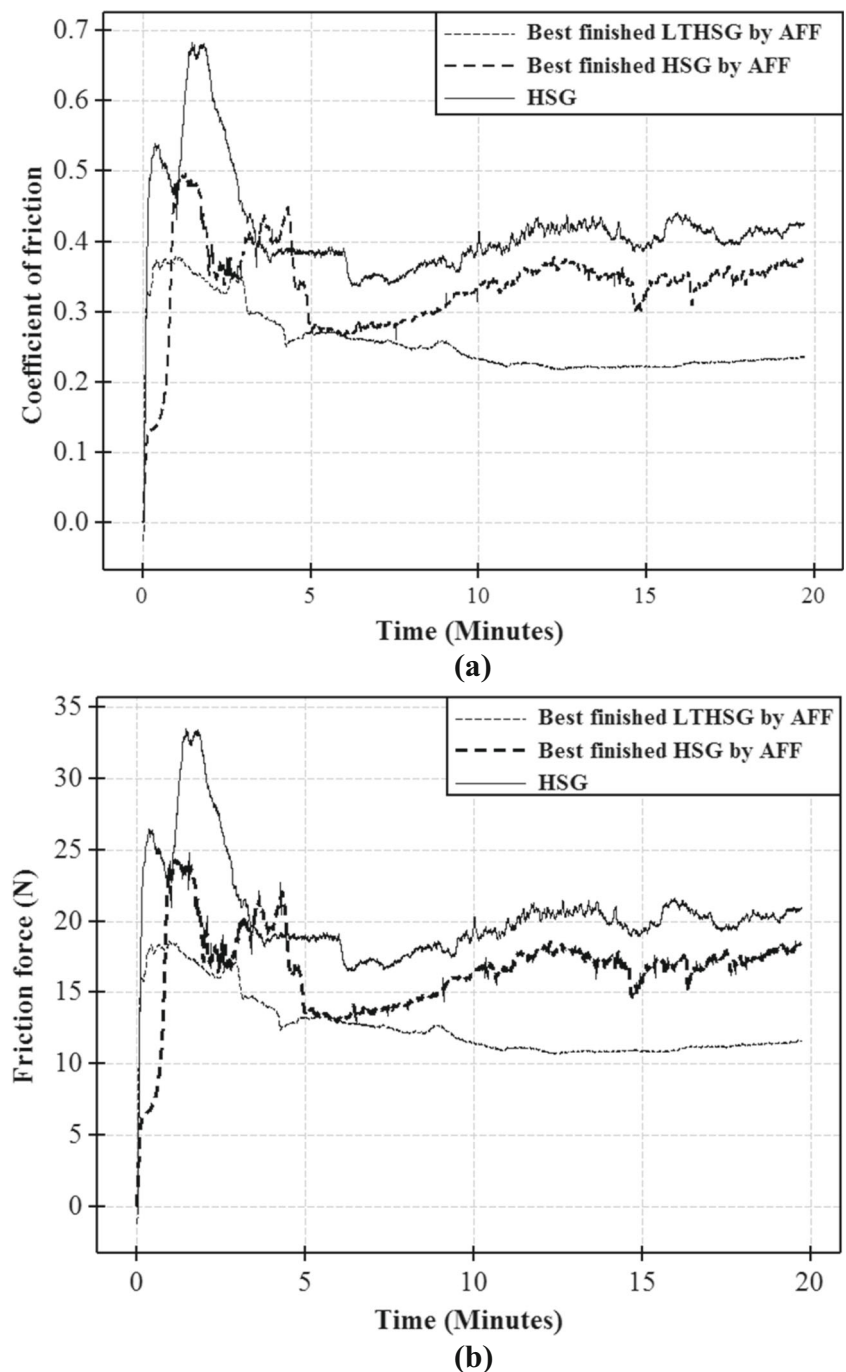
Figure 12 depicts SEM micrographs showing microstructure of the worn flank surfaces of HSG (Fig. 12a), the best finished HSG by AFF (Fig. 12b), and the best finished LTHSG by AFF (Fig. 12c). SEM image of Fig. 12a shows that flank surface of HSG was severely worn with a displacement of material from the wear track and excessive pilling of the worn debris at the edges of the wear track. Worn flank surface of the best finished HSG (Fig. 12b) shows less material displacement, worn debris, and small pilling of the worn debris at the edges of wear track, whereas the worn flank surface of the best finished LTHSG (Fig. 12c) depicts least amount of material displacement and worn debris, and no pilling of the worn debris at the edges of the wear track. Material displacement and its pilling in all three cases indicate severe scuffing wear feature.

5 Conclusions

The following conclusions can be drawn from the present work:

- Laser power and number of passes significantly influence homothetic texture on flank surfaces of the hobbed spur gears in a direction perpendicular to the lay pattern generated by hobbing. Combination of 20 W as power of the fiber laser and 5 number of passes were found to be the optimum values in the present study.
- Generation of laser texture over the hobbing process lay profile creates a mesh-like pattern which makes active abrasive particles to travel in a curved path over the flank surface of LTHSG, thus coveing more distance. This results in more abrasion yielding higher improvement in total profile deviation, total lead deviation, total pitch deviation, radial runout, surface finish, microhardness, and wear resistance during finishing of LTHSG by AFF. It improves wear resistance and microhardness without any thermal damage to the flank surfaces of a gear.
- Finishing of LTHSG by AFF yielded more percentage improvement in profile deviation (24%), lead deviation (3.15%), pitch deviation (35.81%), runout (18.12%), average surface roughness (11.35%), maximum surface roughness (30.15%), microhardness (12%), wear resistance (26.41%), and MRR (24.24%) than the HSG finished by AFF.
- Microstructure of AFF finished LTHSG reveals it possessing smoother flank surfaces which are free from hobbing cutter marks, cracks, pits, and burrs produced

Fig. 11 Variation of (a) coefficient of friction and (b) friction force, with time during fretting wear test of flank surface of the HSG and the best finished HSG and LTHSG by AFF



than AFF finished HSG. The finishing action in both cases is due to abrading action of abrasive particle followed by micro-cutting and micro-plowing.

- AFF process improves microhardness of LTHSG more than that of HSG due to continuous impact of the abrasive particles caused by extrusion pressure and formation of subgrain boundaries which block plastic flow of material.
- The best finished LTHSG has lesser wear rate and more wear resistance due to smoother surface with less variation

in roughness profile and distortion of lattice structure at microscale which forms compressive residual stresses. Smoother surface also results in generation of less heat during power transmission, thus reducing operating temperature of the gear drive. It also has very small value of wear volume which will enhance its service life and mechanical efficiency.

- Fixture design is a very important aspect while finishing the gear by AFF to get a preferred improvement because it provides selective restriction between the workpiece gear

Table 4 Results of fretting wear test for the HSG and the best finished HSG and LTHSG by AFF process

Parameter name (unit)	HSG	Best finished HSG by AFF	Best finished LTHSG by AFF
Max. value of frictional force (<i>N</i>)	33.48	24.35	18.64
Max. value of coefficient of friction	0.683	0.497	0.379
Wear volume <i>V</i> (mm ³)	0.174	0.0675	0.0496
Specific wear rate <i>k</i> (mm ³ /Nm)	14.8×10^{-6}	5.73×10^{-6}	4.22×10^{-6}
Wear rate (mm ³ /m)	7.4×10^{-4}	2.86×10^{-4}	2.11×10^{-4}

and the fixture. Improvement in responses can be increased by suitably modifying design of the fixture.

- LT-AFF is an effective process to improve microgeometry, surface quality, and MRR of AFF process for gear finishing. It does not require any changes in the AFF

apparatus and fixture unlike other hybrid variants of AFF because laser texturing is being done prior to gear finishing by AFF. This makes LT-AFF effective and economical in terms of non-requirement of modification of AFF apparatus and productive process to improve

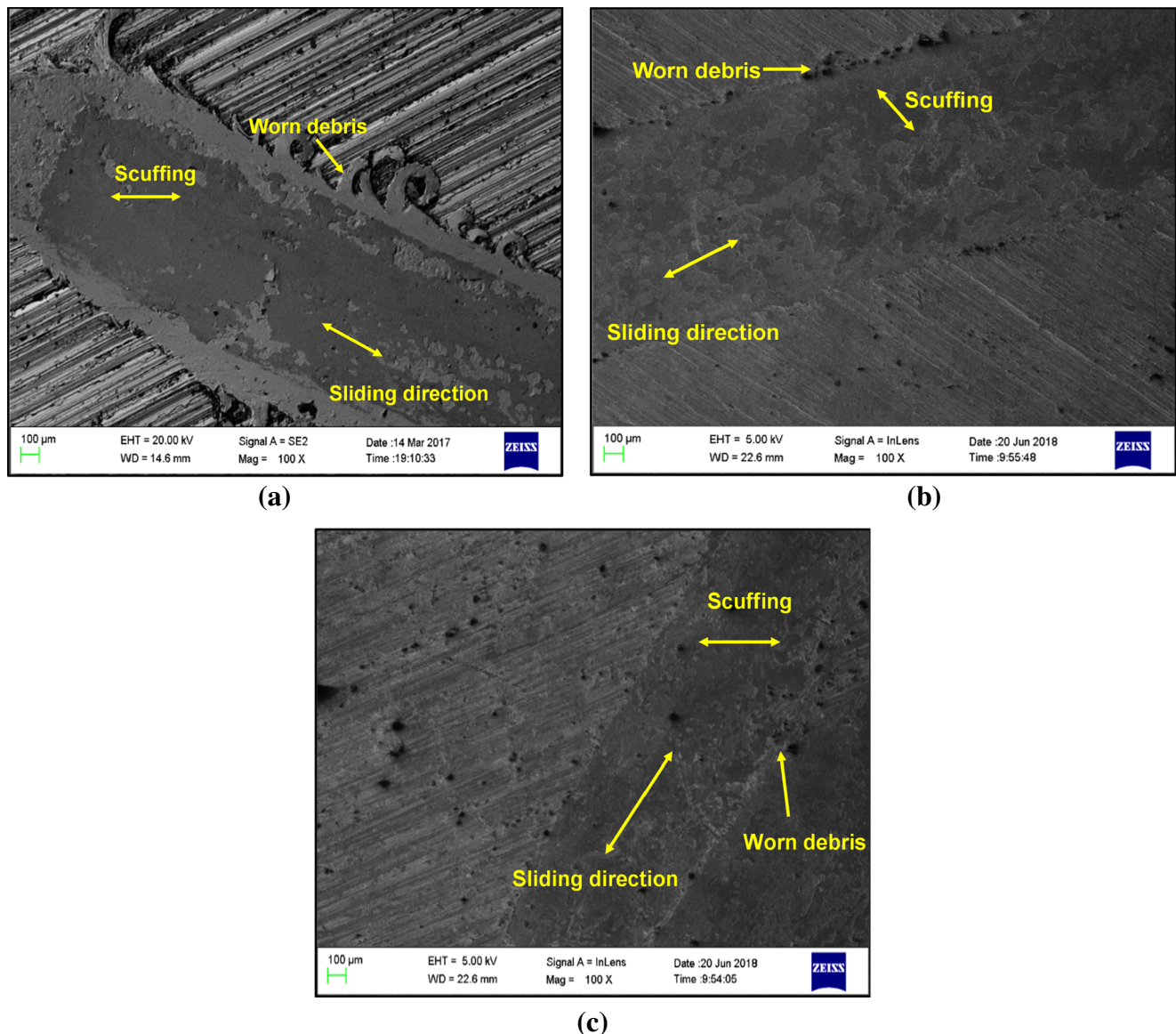


Fig. 12 SEM images of the worm flank surface of the (a) HSG, (b) best finished HSG by AFF, and (c) best finished LTHSG by AFF

microgeometry, surface finish, and MRR in AFF process for gear finishing.

Publisher's Note Springer Nature remains neutral with regard to jurisdictional claims in published maps and institutional affiliations.

References

- Maitra GM (2001) Handbook of gear design. Tata McGraw-Hill Publishing Company Limited, New Delhi
- Chaubey SK, Jain NK (2017) Investigations on microgeometry of meso bevel and meso helical gears manufactured by WEDM process. *Int J Adv Manuf Technol* 93(9):4217–4231. <https://doi.org/10.1007/s00170-017-0884-y>
- Radzevich SP (2012) Dudley's handbook of practical gear design and manufacture. CRC Press, New York
- Jain NK, Petare AC (2016) In: Hashmi MSJ (ed) Review of gear finishing processes, Chapter 1.4 in *Comprehensive Materials Finishing*, vol 1. Elsevier, Oxford, pp 93–120. <https://doi.org/10.1016/B978-0-12-803581-8.09150-5>
- Shaikh JH, Jain NK, Venkatesh VC (2013) Precision finishing of bevel gears by electrochemical honing. *Mater Manuf Process* 28(10):1117–1123. <https://doi.org/10.1080/10426914.2013.811737>
- Pathak S, Jain NK, Palani IA (2014) On use of pulsed electrochemical honing to improve micro-geometry of bevel gears. *Mater Manuf Process* 29(11–12):1461–1469. <https://doi.org/10.1080/10426914.2014.952032>
- Xu YC, Zhang KH, Lu S, Liu ZQ (2013) Experimental investigations into abrasive flow machining of helical gear. *Key Eng Mater* 546:65–69. <https://doi.org/10.4028/www.scientific.net/KEM.546.65>
- Venkatesh G, Sharma AK, Singh N, Kumar P (2014) Finishing of bevel gears using abrasive flow machining. *Proce Eng* 97:320–328. <https://doi.org/10.1016/j.proeng.2014.12.255>
- Petare AC, Jain NK (2018a) Improving spur gear microgeometry and surface finish by AFF process. *Mater Manuf Process* 33(9):923–934. <https://doi.org/10.1080/10426914.2017.1376074>
- Petare AC, Jain NK (2018b) On simultaneous improvement of wear characteristics, surface finish and microgeometry of straight bevel gears by abrasive flow finishing process. *Wear* 404–405:38–49. <https://doi.org/10.1016/j.wear.2018.03.002>
- Venkatesh G, Sharma AK, Kumar P (2015) On ultrasonic assisted abrasive flow finishing of bevel gears. *Int J Mach Tools Manuf* 89:29–38. <https://doi.org/10.1016/j.ijmactools.2014.10.014>
- Petare AC, Jain NK (2018c) A critical review of past research and advances in abrasive flow finishing process. *Int J Adv Manuf Technol* 97(1):741–782. <https://doi.org/10.1007/s00170-018-1928-7>
- Firdaus SBA, Jameelah GM, Juyana AW (2016) Laser surface texturing and its contribution to friction and wear reduction: a brief review. *Ind Lub Trib* 68(1):57–66. <https://doi.org/10.1108/ILT-05-2015-0067>
- Sasi R, Kanmani SS, Palani IA (2017) Performance of laser surface textured high speed steel cutting tool in machining of Al7075-T6 aerospace alloy. *Surf Coat Technol* 313:337–346. <https://doi.org/10.1016/j.surfcoat.2017.01.118>
- Kang Z, Fu Y, Ji J, Puoza JC (2017) Effect of local laser surface texturing on tribological performance of injection cam. *Int J Adv Manuf Technol* 92(5):1751–1760. <https://doi.org/10.1007/s00170-017-0227-z>
- Ye D, Lijun Y, Bai C, Xiaoli W, Yang W, Hui X (2018) Investigations on femtosecond laser-modified microgroove-textured cemented carbide YT15 turning tool with promotion in cutting performance. *Int J Adv Manuf Technol* 96(9):4367–4379. <https://doi.org/10.1007/s00170-018-1906-0>
- Hao X, Chen X, Xiao S, Li L, He N (2018) Cutting performance of carbide tools with hybrid texture. *Int J Adv Manuf Technol* 97:3547–3556. <https://doi.org/10.1007/s00170-018-2188-2>
- Singh A, Patel DS, Ramkumar J, Balani K (2018) Single step laser surface texturing for enhancing contact angle and tribological properties. *Int J Adv Manuf Technol*. <https://doi.org/10.1007/s00170-018-1579-8>
- Niketh S, Samuel GL (2017) Surface texturing for tribology enhancement and its application on drill tool for the sustainable machining of titanium alloy. *J Clean Prod* 167:253–270. <https://doi.org/10.1016/j.jclepro.2017.08.178>
- Xing Y, Deng J, Feng X, Yu S (2013) Effect of laser surface texturing on Si3N4/TiC ceramic sliding against steel under dry friction. *Mater Des* 52:234–245. <https://doi.org/10.1016/j.matdes.2013.05.077>
- ASTM G133–05 (2016) Standard test method for linearly reciprocating ball-on-flat sliding wear. ASTM International, West Conshohocken <https://www.astm.org/Standards/G133.htm>. Accessed on 09 Jul 2018
- Archard JF (1953) Contact and rubbing of flat surfaces. *Appl Phys* 24:981–988
- ASTM E92–82 (2003) Standard test method for vickers hardness of metallic materials. ASTM International, West Conshohocken <https://www.astm.org/DATABASE.CART/HISTORICAL/E92-82R03.htm>. Accessed on 09 Jul 2018
- Dai FZ, Geng J, Tan WS, Ren XD, Lu JZ, Huang S (2018) Friction and wear on laser textured Ti6Al4V surface subjected to laser shock peening with contacting foil. *Opt Laser Technol* 103:142–150. <https://doi.org/10.1016/j.optlastec.2017.12.04>
- Sankar MR, Jain VK, Ramkumar J (2009) Experimental investigations into rotating workpiece abrasive flow finishing. *Wear* 267(1):43–51. <https://doi.org/10.1016/j.wear.2008.11.007>
- Pathak S, Jain NK, Palani IA (2015) On surface quality and wear resistance of straight bevel gears processed by pulsed electrochemical honing process. *Int J Electrochem Sci* 10(11):8869–8885